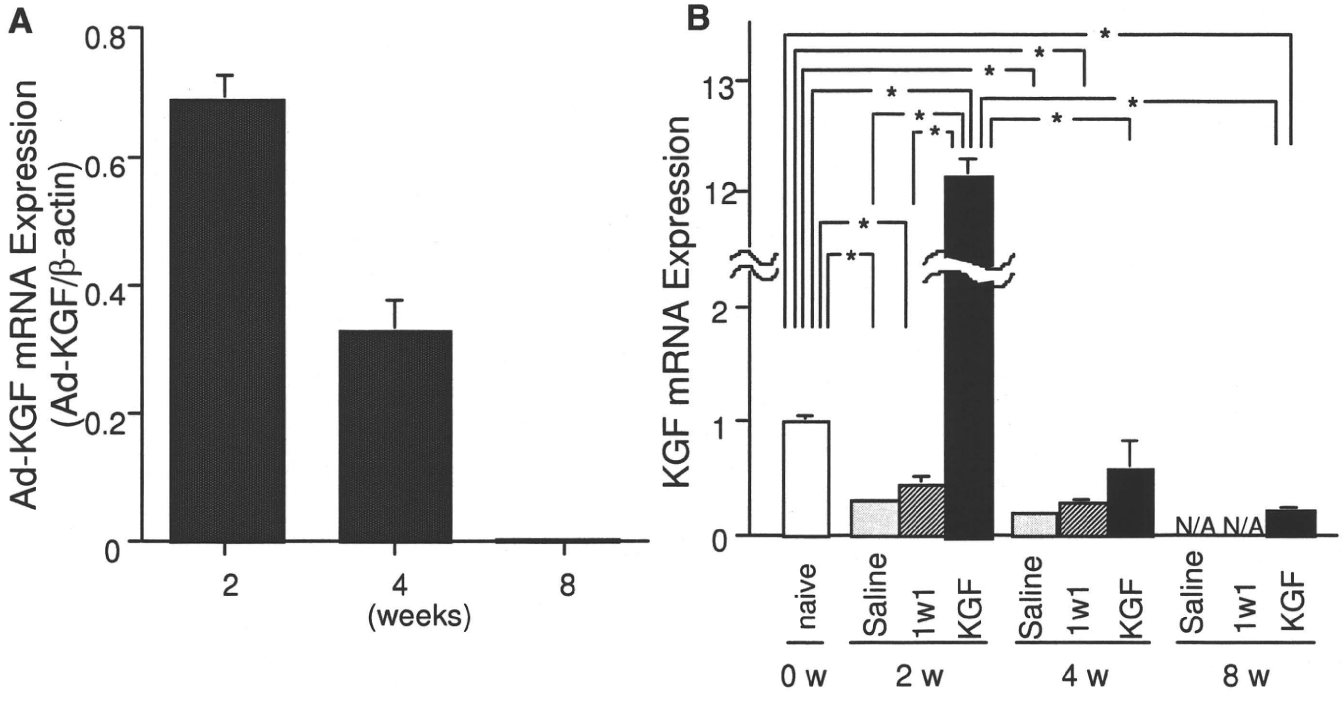
A
Ad-KGF mRNA Expression
(Ad-KGF/β-actin)
0.8
0.6
0.4
0.2
0
2
4
8
(weeks)
B
KGF mRNA Expression
13
12
2
1
0
N/A N/A
naive
Saline
1w1
KGF
Saline
1w1
KGF
Saline
1w1
KGF
0 w
2 w
4 w
8 w

Fig. 6

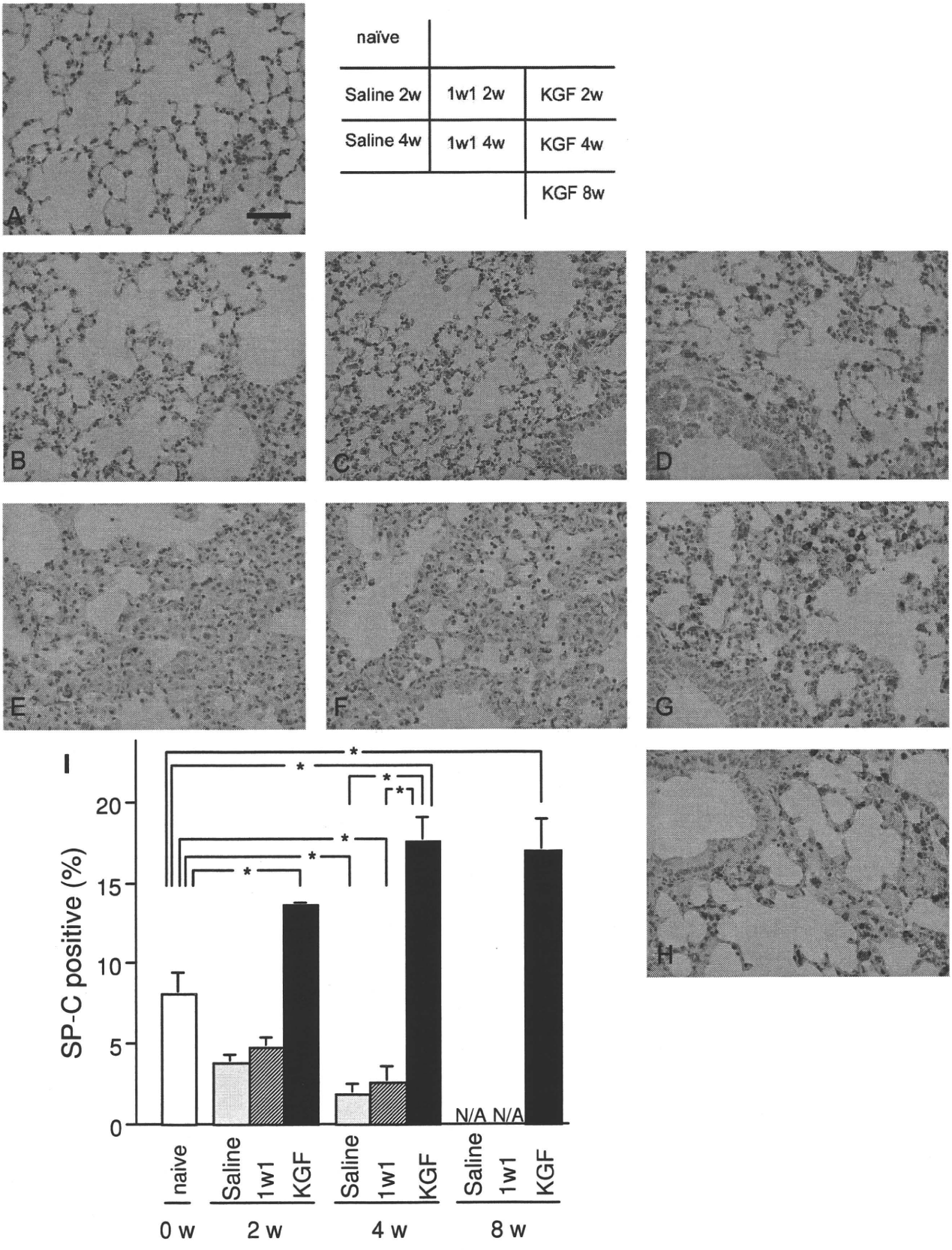
naïve
Saline 2w
1w1 2w
KGF 2w
Saline 4w
1w1 4w
KGF 4w
KGF 8w
A
B
C
D
E
F
G
H
I
SP-C positive (%)
20
15
10
5
0
N/A N/A
naive
Saline
1w1
KGF
Saline
1w1
KGF
Saline
1w1
KGF
0 w
2 w
4 w
8 w

Fig. 7

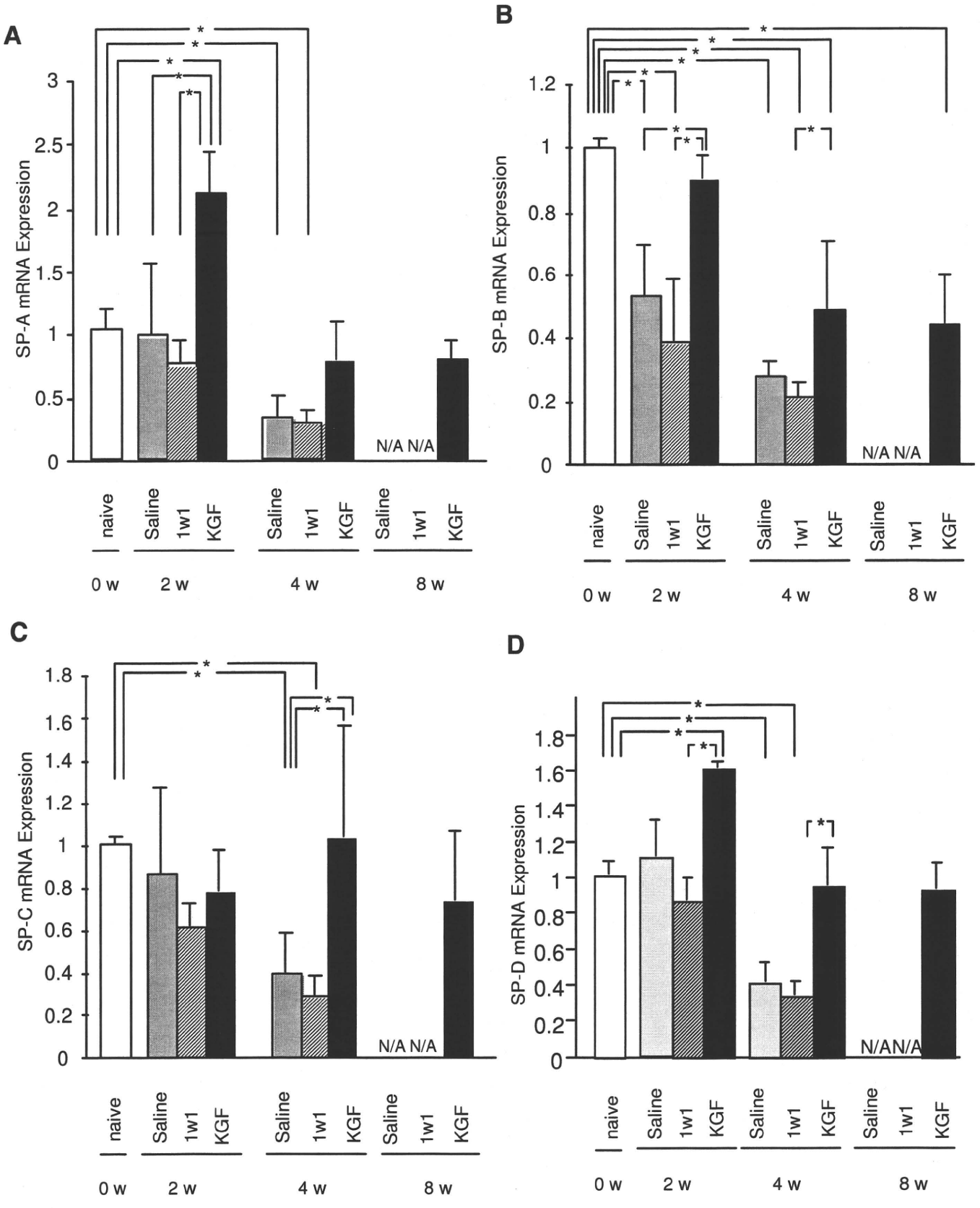
A
SP-A mRNA Expression
3
2.5
2
1.5
1
0.5
0
N/A N/A
naive
Saline
1w1
KGF
Saline
1w1
KGF
Saline
1w1
KGF
0 w
2 w
4 w
8 w
B
SP-B mRNA Expression
1.2
1
0.8
0.6
0.4
0.2
0
N/A N/A
naive
Saline
1w1
KGF
Saline
1w1
KGF
Saline
1w1
KGF
0 w
2 w
4 w
8 w
C
SP-C mRNA Expression
1.8
1.6
1.4
1.2
1
0.8
0.6
0.4
0.2
0
N/A N/A
naive
Saline
1w1
KGF
Saline
1w1
KGF
Saline
1w1
KGF
0 w
2 w
4 w
8 w
D
SP-D mRNA Expression
1.8
1.6
1.4
1.2
1
0.8
0.6
0.4
0.2
0
N/AN/A
naive
Saline
1w1
KGF
Saline
1w1
KGF
Saline
1w1
KGF
0 w
2 w
4 w
8 w

Fig. 8

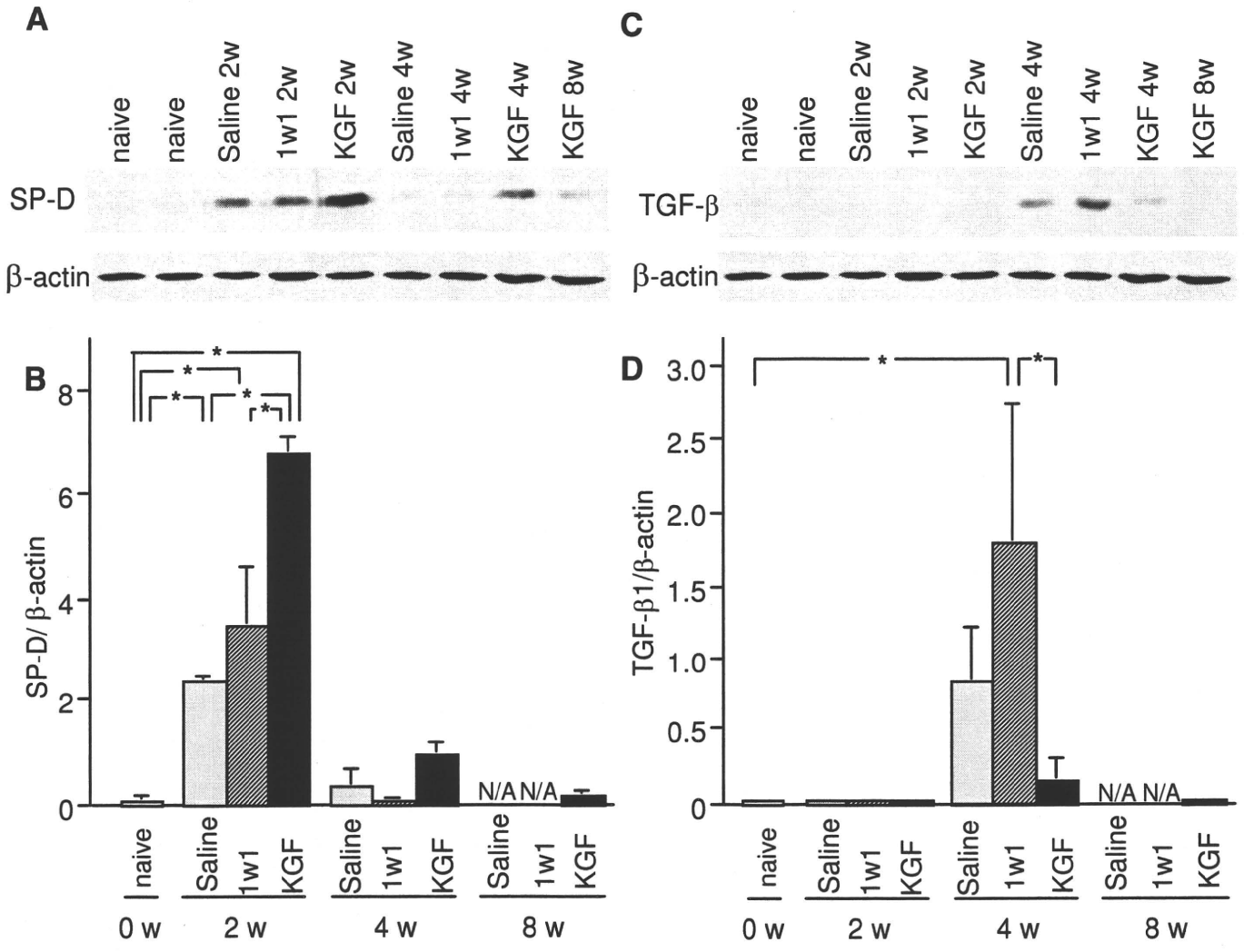
A
naive
naive
Saline 2w
1w1 2w
KGF 2w
Saline 4w
1w1 4w
KGF 4w
KGF 8w
SP-D
β-actin
C
naive
naive
Saline 2w
1w1 2w
KGF 2w
Saline 4w
1w1 4w
KGF 4w
KGF 8w
TGF-β
β-actin
B
SP-D/ β-actin
0
2
4
6
8
*
*
*
*
*
N/A N/A
naive
Saline
1w1
KGF
Saline
1w1
KGF
Saline
1w1
KGF
0 w
2 w
4 w
8 w
D
TGF-β1/β-actin
0
0.5
1.0
1.5
2.0
2.5
3.0
*
*
N/A N/A
naive
Saline
1w1
KGF
Saline
1w1
KGF
Saline
1w1
KGF
0 w
2 w
4 w
8 w

Fig. 9

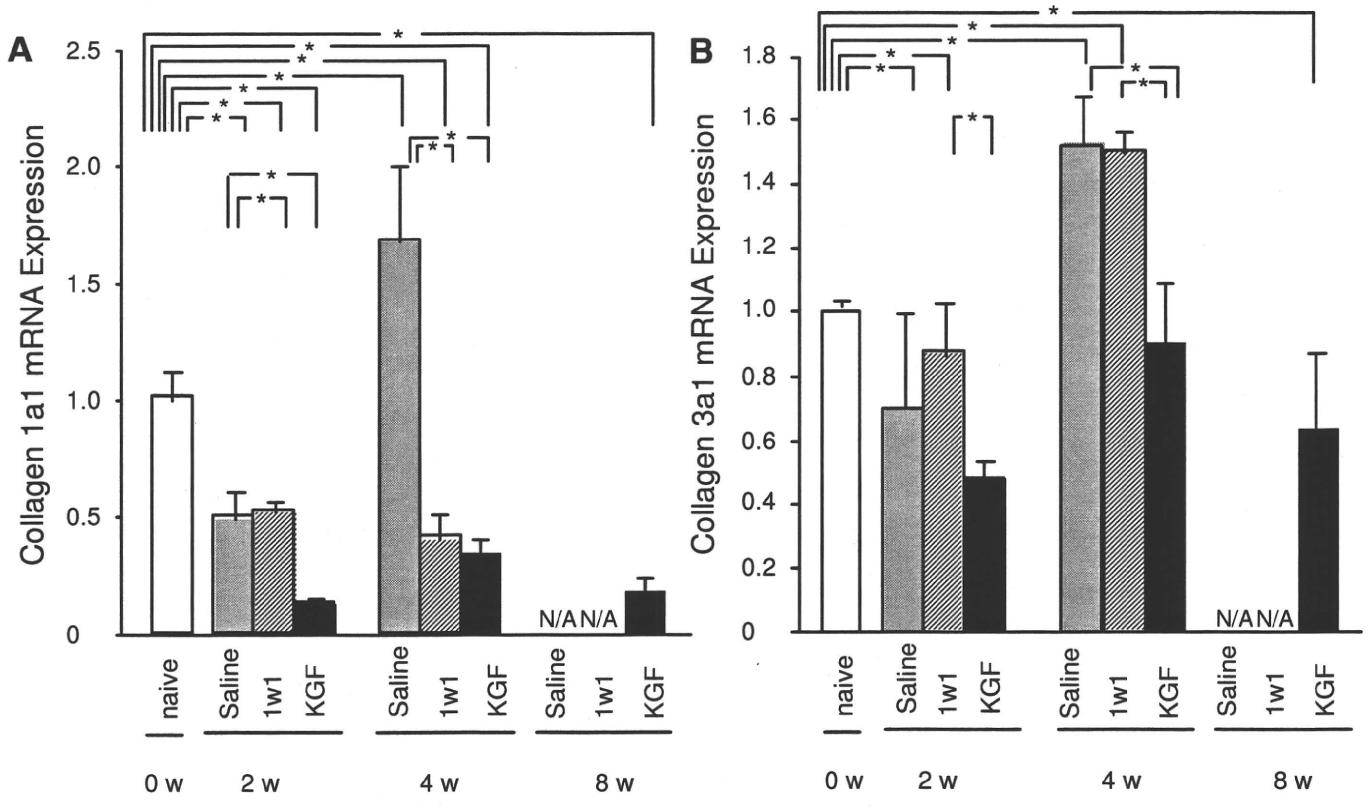
A
Collagen 1a1 mRNA Expression
2.5
2.0
1.5
1.0
0.5
0
N/A N/A
naive
Saline
1w1
KGF
Saline
1w1
KGF
Saline
1w1
KGF
0 w
2 w
4 w
8 w
B
Collagen 3a1 mRNA Expression
1.8
1.6
1.4
1.2
1.0
0.8
0.6
0.4
0.2
0
N/A N/A
naive
Saline
1w1
KGF
Saline
1w1
KGF
Saline
1w1
KGF
0 w
2 w
4 w
8 w

Fig. 10

Online data supplement

Keratinocyte growth factor gene transduction ameliorates pulmonary fibrosis induced by bleomycin in mice

Seiko Sakamoto[1], Takuya Yazawa[2], Yasuko Baba[1], Hanako Sato[2], Yumi Kanegae[3], Toyohiro Hirai[4], Izumu Saito[3], Takahisa Goto[1], Kiyoyasu Kurahashi[1]

Materials and Methods

Generation of recombinant adenovirus

We used a recombinant adenovirus (rAd) expressing murine KGF cDNA under the control of a potent CAG promoter (23) (AxCAmKGF denoted Ad-KGF in this paper), which was previously reported (22) (Fig. 1-i). The absence of contamination by replication-competent adenovirus (RCA) was confirmed by PCR of the E1 region sequence. Ax1w1, which bears no insert, including any promoter, cDNA, or poly(A) sequence (24), denoted Ad-1w1 in this paper was used as a control (Fig. 1-ii). Purified and concentrated viral stocks were prepared as described previously (E1).

Experimental protocol

All protocols for the animal experiments were approved by the Animal Research Committee of Yokohama City University (Yokohama, Japan). C57BL6 mice (male, 10 weeks) were purchased from Charles River Japan (Yokohama, Japan). Bleomycin was supplied by Nippon Kayaku (Tokyo, Japan). On Day 1, mice were anesthetized with isoflurane, xylazine, and ketamine, and a 7-day micro-osmotic pump (ALZET, 1007D, Durect, Cupertino, CA) containing 120 mg/kg of bleomycin was aseptically implanted into a subcutaneous space. On Day 8, mice were again anesthetized, and saline or 1.0 x 10^9 plaque-forming units (PFU) of an adenoviral vector, either Ad-KGF or Ad-1w1, was instilled intratracheally using a MicroSprayer (Penn-Century, Philadelphia, PA). In a survival trial, one group of mice received the lower dose of 1.0 x 10^8 PFU of the adenoviral vector. The choice of the 7-d interval between the start of bleomycin and administration of Ad-KGF was based on the study by Chaudhary *et al.* that demonstrated that the transition from the inflammatory to the fibrotic phase after bleomycin administration occurs in about 9 d in mice (E2). Our preliminary experiments showed that,

unlike pulmonary fibrosis in humans, which is mostly irreversible, pulmonary fibrosis induced by a single administration of bleomycin in mice was progressive up to 4 weeks but spontaneously tended to diminish thereafter. Therefore, a second osmotic pump containing 120 mg/kg of bleomycin was implanted on Day 29 to induce pulmonary fibrosis progressively for 8 weeks. Another set of animals (naïve group) received neither bleomycin nor the vector. On Day 56, mice were anesthetized, and pulmonary function was measured using a computer-controlled animal ventilator. Mice were then euthanized under deep anesthesia, and both lungs were harvested through a thoracotomy for histopathological examination, RNA extraction for PCR, and homogenization for Western blotting. One group of mice was used to evaluate the effects of adenovirus vectors on unaffected mice (without bleomycin pretreatment). Lungs of mice harvested 1 or 3 weeks after the administration of Ad-KGF were processed for histopathological examination.

Survival study

Mice were given bleomycin and the viral vector as described above (n = 15 to 16 in each group). Survival was then assessed for up to 8 weeks. Throughout this time period, the animals had free access to water and food.

Histopathological examination

Excised lungs were fixed with 4% paraformaldehyde in PBS for 48 h for histologic examination. The fixed lungs were embedded in paraffin. Four-micrometer-thick paraffin sections were dewaxed and stained with hematoxylin and eosin (H&E) for routine histopathological examination. To visualize collagen deposition clearly, we stained another set of sections with Masson's trichrome.

Histopathological quantification of fibrosis

The Ashcroft score was calculated for semiquantitative analysis of fibrotic change (25). In brief, each lung section was placed over 2 mm square grids. Grids that contained more than 50% alveolar tissue were selected and observed at a magnification of 100. Each field was individually assessed for the severity of fibrotic change and allotted a score from 0 (normal) to 8 (total fibrosis) using a predetermined scale of severity (25). After examination of the whole section, the average of the scores from all fields

was taken as the fibrosis score. Each specimen was scored independently by two investigators who were blinded to the treatment, and the mean of their individual scores was considered the fibrosis score of the sample.

Immunohistochemistry of lungs

Four-micrometer-thick paraffin sections were immunostained with KGF (FGF-7) antibody (sc7882, Santa Cruz Biotechnology, Santa Cruz, CA) and rabbit polyclonal anti-surfactant protein C (SP-C) antibody (sc-13979, Santa Cruz Biotechnology), followed by processing using an EnVision System (Dako, Glostrup, Denmark) according to the manufacturer's instruction. To detect KGF, the antigen in the sections was retrieved by autoclaving at 120°C for 15 min. Sections were briefly incubated with 0.03% hydrogen peroxide to eliminate endogenous peroxidase. The non-specific staining was blocked with a serum-free blocking reagent (X0909, Dako). The primary antibodies were diluted at 1:100 using Antibody Diluent (Dako). After washing in PBS, the sections were incubated for 30 min with a labeled polymer (K5027, EnVision System, Dako), and the signals were colorized with diaminobenzidine (DAB). Nuclei were counterstained with hematoxylin. Cells positive for SP-C were counted in three different parts of the section in a blinded manner and are presented as a percentage of the total number of cells in the field.

Measurement of pulmonary function

Mice were anesthetized with xylazine and ketamine, and the trachea was cannulated by a metallic needle (1.20 mm inner diameter, 4 mm long) through a tracheostomy. Mice were ventilated with a tidal volume of 8 ml/kg at a rate of 150 breaths/min, and pulmonary function was measured using a computer-controlled animal ventilator (flexiVENT, Scireq, Montreal, Canada). Quasi-static deflation pressure-volume (P-V) curves were collected with a positive end-expiratory pressure (PEEP) of 3 hPa to measure quasi-static compliance (Cst). Functional residual capacity (FRC) and total lung capacity (TLC) were defined as the lung volume at 3 hPa and 25 hPa, respectively (E3). The lung volume (TLC - FRC) was calculated as the volume of air required to inflate lungs from FRC to TLC.

Reverse transcriptase polymerase chain reaction (PCR)

Total RNA was extracted from the lungs using TRizol (Invitrogen, Carlsbad, CA) and cDNA synthesis

was performed using a PrimeScript High Fidelity RT-PCR kit (Takara Bio, Shiga, Japan); subsequent PCR reactions were performed using an RNA-LAPCR kit (Takara Bio) according to the manufacturer's instructions. β-Actin served as the internal control. The number of PCR cycles was set at 35 for Ad-KGF and at 25 for β-actin. The forward and reverse primer sequences for Ad-KGF and β-actin are listed in Table E1. Densitometry scanning was performed using NIH Image software (National Institute of Health, Rockville, MD).

Real-time PCR

Total RNA (to 100 ng) was transcribed using Superscript III reverse transcriptase (Invitrogen) and oligo-(dT). PCR amplification was performed on a Thermal Cycler Dice (Takara Bio) using SYBR Green I as a double-strand DNA-specific binding dye and continuous fluorescence monitoring according to the manufacturer's instructions. The forward and reverse primer sequences for each mRNA are listed in Table E2. β-Actin was used as the assay standard. The levels of expression of each mRNA and their estimated crossing points were determined relative to the standard preparation using the Thermal Cycler Dice computer software (Takara Bio). Expression data were normalized based on the expression levels of β-actin mRNA.

Western blotting for transforming growth factor (TGF)-β1 and SP-D

One lobe of the right lung was homogenized with an elution buffer containing 20 mM HEPES, pH 7.6, 20 mM NaCl, 0.5 mM EDTA, and 10% glycerol on ice. Standardized quantities of proteins were loaded onto SDS-PAGE gel and transferred electrophoretically onto nitrocellulose membranes. After the membranes were blocked with 0.5% skim milk in phosphate-buffered saline/0.1% Tween 20 (PBS-T), they were incubated with diluted primary antibody in PBS-T containing 0.5% skim milk for 1 h. The dilutions of primary antibodies were 1:2000 for TGF-β1, 1:2000 for SP-D, and 1:10000 for β-actin. Primary antibodies of TGF-β1 and SP-D were obtained from Santa Cruz Technology. The membranes were washed three times in PBS-T for 15 min and incubated for 30 min with peroxidase-conjugated IgG. After membranes were washed three times in PBS-T for 15 min, specific signals were visualized using an ECL system (GE Healthcare Life Science, Amersham, UK) and blots were exposed on X-ray films.

Statistics

Data are reported as means and SEM for each group. Comparisons of multiple groups were made with a Tukey-Kramer *post hoc* test after analysis of variance (ANOVA). Survival rates are shown on the basis of Kaplan-Meier product limit curves, and the groups were compared by log rank test. A $p < 0.05$ was considered significant.

References

E1. Kanegae Y, Makimura M, Saito I. A simple and efficient method for purification of infectious recombinant adenovirus. Jpn J Med Sci Biol 1994;47:157-166.

E2. Chaudhary NI, Schnapp A, Park JE: Pharmacologic differentiation of inflammation and fibrosis in the rat bleomycin model. Am J Respir Crit Care Med 2006;173:769-776.

E3. Hirai T, Hosokawa M, Kawakami K, Takubo Y, Sakai N, Oku Y, Chin K, Ohi M, Higuchi K, Kuno K, Mishima M. Age-related changes in the static and dynamic mechanical properties of mouse lungs. Respir Physiol. 1995;102:195-203.

Tables

Table E1. Primer sequences for RT-PCR

Gene	Forward primer	Reverse primer
β-actin	5'-GGCCAACCGTGAAAAGATGAC	5'-ATTGCCGATAGTGATGACCTG
Ad-mKGF	5'-GACCCAGGAGATGAAGAA	5'-CTAGACTAGTTTAATTAA

Ad-mKGF, adenovirus vector for murine keratinocyte growth factor

Table E2. Primer sequences for SYBR-green-based real-time PCR

Gene	Forward primer	Reverse primer
β-actin	5'-CATCCGTAAAGACCTCTATGCCAAC	5'-ATGGAGCCACCGATCCACA
KGF	5'-TGGTACCTGAGGATTGACAAACGA	5'-CCTTTGATTGCCACAATTCCAAC
SP-A	5'-CTCGGAGGCAGACATCCACA	5'-TGATGCCAGCAACAACAGTCAA
SP-B	5'-GAGTGTGCACAAGGCCCTCA	5'-CCTCACACTCTTGGCACAGGTC
SP-C	5'-CATCATGAAGATGGCTCCAGAGA	5'-ACACAGGGTGCTCACAGCAAG
SP-D	5'- CCTCAAGGCAAACCAGGTCCTA	5'-TGCATGCCAGGAGCACCTAC
Col 1a	5'-CAGGGTATTGCTGGACAACGTG	5'-GGACCTTGTTTGCCAGGTTCA
Col 3a	5'-CCACGTAAGCACTGGTGGACA	5'-GCCAGCTGCACATCAACGA

KGF, keratinocyte growth factor; SP, surfactant protein; Col, collagen

Figure Legends

Figure E1. Representative microphotographs of bleomycin-induced subpleural inflammation in the saline (A), 1w1 (B), and KGF (C) groups 2 weeks after bleomycin administration and 1 week after saline, Ad-1w1, or Ad-KGF instillation, respectively. Intra-alveolar inflammatory cell infiltration was not considerably different among the three groups (hematoxylin and eosin stain). Black bars, 100 mm.

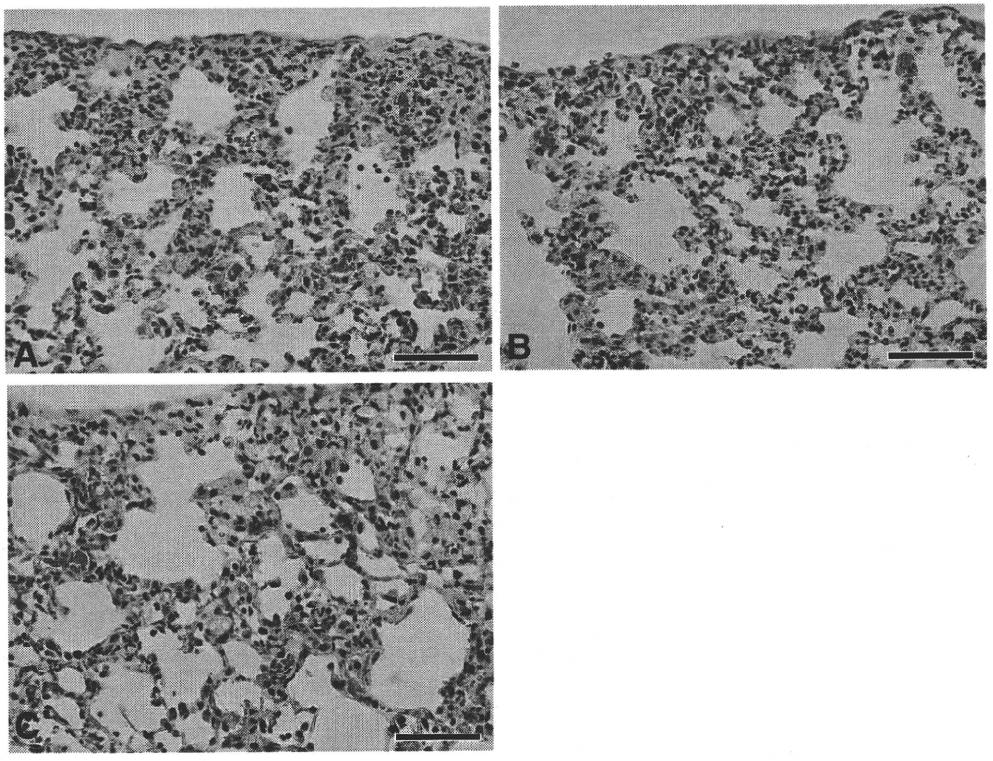

Fig. E1

JOURNAL OF VIROLOGY, Jan. 2010, p. 303–311 Vol. 84, No. 1
0022-538X/10/$12.00 doi:10.1128/JVI.01448-09

Pathogenesis of Hepatitis C Virus Infection in *Tupaia belangeri*▽†

Yutaka Amako,[1] Kyoko Tsukiyama-Kohara,[1,2] Asao Katsume,[1,3] Yuichi Hirata,[1] Satoshi Sekiguchi,[1] Yoshimi Tobita,[1] Yukiko Hayashi,[4] Tsunekazu Hishima,[4] Nobuaki Funata,[4] Hiromichi Yonekawa,[5] and Michinori Kohara[1]*

Department of Microbiology and Cell Biology, Tokyo Metropolitan Institute of Medical Science, 2-1-6, Kamikitazawa, Setagaya-ku, Tokyo 156-0057, Japan[1]; Department of Experimental Phylaxiology, Faculty of Medical and Pharmaceutical Sciences, Kumamoto University, 1-1-1 Honjo Kumamoto City, Kumamoto 860-8556, Japan[2]; Fuji Gotemba Research Laboratory, Chugai Pharmaceutical Company, Ltd., 135, Komakado 1 Chome, Gotemba-shi, Shizuoka 412-8513, Japan[3]; Department of Pathology, Tokyo Metropolitan Komagome Hospital, 3-18-22 Honkomagome, Bunkyo-ku, Tokyo 113-8677, Japan[4]; and Laboratory of Animal Science, Tokyo Metropolitan Institute of Medical Science, 2-1-6, Kamikitazawa, Setagaya-ku, Tokyo 156-0057, Japan[5]

Received 14 July 2009/Accepted 5 October 2009

The lack of a small-animal model has hampered the analysis of hepatitis C virus (HCV) pathogenesis. The tupaia (*Tupaia belangeri*), a tree shrew, has shown susceptibility to HCV infection and has been considered a possible candidate for a small experimental model of HCV infection. However, a longitudinal analysis of HCV-infected tupaias has yet to be described. Here, we provide an analysis of HCV pathogenesis during the course of infection in tupaias over a 3-year period. The animals were inoculated with hepatitis C patient serum HCR6 or viral particles reconstituted from full-length cDNA. In either case, inoculation caused mild hepatitis and intermittent viremia during the acute phase of infection. Histological analysis of infected livers revealed that HCV caused chronic hepatitis that worsened in a time-dependent manner. Liver steatosis, cirrhotic nodules, and accompanying tumorigenesis were also detected. To examine whether infectious virus particles were produced in tupaia livers, naive animals were inoculated with sera from HCV-infected tupaias, which had been confirmed positive for HCV RNA. As a result, the recipient animals also displayed mild hepatitis and intermittent viremia. Quasispecies were also observed in the NS5A region, signaling phylogenic lineage from the original inoculating sequence. Taken together, these data suggest that the tupaia is a practical animal model for experimental studies of HCV infection.

Hepatitis C virus (HCV) is a small enveloped virus that causes chronic hepatitis worldwide (32). HCV belongs to the genus *Hepacivirus* of the family *Flaviviridae*. Its genome comprises 9.6 kb of single-stranded RNA of positive polarity flanked by highly conserved untranslated regions at both the 5′ and 3′ ends (4, 27, 29). The 5′ untranslated region harbors an internal ribosomal entry site (29) that initiates translation of a single open reading frame encoding a large polyprotein comprising about 3,010 amino acids (35). The encoded polyprotein is co- and posttranslationally processed into 10 individual viral proteins (15).

In most cases of human infection, HCV is highly potent and establishes lifelong persistent infection, which progressively leads to chronic hepatitis, liver steatosis, cirrhosis, and hepatocellular carcinoma (9, 16, 21). The most effective therapy for treatment of HCV infection is administration of pegylated interferon combined with ribavirin. However, the combination therapy is an arduous regimen for patients; furthermore, HCV genotype 1b does not respond efficiently (19). The prevailing scientific opinion is that a more viable option than interferon treatment is needed.

The chimpanzee is the only validated animal model for in vivo studies of HCV infection, and it is capable of reproducing most aspects of human infection (5, 18, 23, 28, 35, 36). The chimpanzee is also the only validated animal for testing the authenticity and infectivity of cloned viral sequences (8, 14, 35, 36). However, chimpanzees are relatively rare and expensive experimental subjects. Cross-species transmission from infected chimpanzees to other nonhuman primates has been tested but has proven unsuccessful for all species evaluated (1).

The tupaia (*Tupaia belangeri*), a tree shrew, is a small nonprimate mammal indigenous to certain areas of Southeast Asia (6). It is susceptible to infection with a wide range of human-pathogenic viruses, including hepatitis B viruses (13, 20, 31), and appears to be permissive for HCV infection (33, 34). In an initial report, approximately one-third of inoculated animals exhibited acute, transient infection, although none developed the high-titer sustained viremia characteristic of infection in humans and chimpanzees (33). The short duration of follow-up precluded any observation of liver pathology. In addition to the putative in vivo model, cultured primary hepatocytes from tupaias can be infected with HCV, leading to de novo synthesis of HCV RNA (37). These reports strongly support tupaias as a valid model for experimental studies of HCV infection. However, longitudinal analyses evaluating the clinical development and pathology of HCV-infected tupaias have yet to be exam-

* Corresponding author. Mailing address: Department of Microbiology and Cell Biology, The Tokyo Metropolitan Institute of Medical Science, 2-1-6, Kamikitazawa, Setagaya-ku, Tokyo 156-0057, Japan. Phone: 81-3-5316-3232. Fax: 81-3-5316-3137. E-mail: kohara-mc@igakuken.or.jp.

† Supplemental material for this article may be found at http://jvi.asm.org/.

▽ Published ahead of print on 21 October 2009.

TABLE 1. Experimental HCV infections performed in this study

Tupaia no.	Inoculum		Biopsy/sacrifice[b]
	Type	Quantity (GE/tupaia)[a]	
Group I[c]			
Tup.4	RCV	1×10^7	84, 94/144 wk p.i.
Tup.5	HCR6	6×10^5	95, 105/155 wk p.i.
Tup.6	HCR6	6×10^5	95, 105/155 wk p.i.
Tup.8	RCV	1×10^7	84, 94/144 wk p.i.
Group II[d]			
Tup.9	Tup.5 (5 wk p.i.)	1×10^2	NT
Tup.10	Tup.5 (5 wk p.i.)	1×10^2	NT
Tup.11	Tup.8 (10 wk p.i.)	1×10^2	NT
Tup.12	Tup.8 (10 wk p.i.)	1×10^2	NT
Tup.13	Tup.4 (8 wk p.i.)	1×10^2	NT
Tup.14	Tup.4 (8 wk p.i.)	1×10^2	NT
Group III[e]			
Tup.15	None		92/100 wk
Tup.17	None		92/100 wk
Tup.38	None		242 wk
Tup.39	None		242 wk

[a] Viral RNA GE/tupaia was estimated by Quantitative real-time RT-PCR (GE, genome equivalents; sensitivity > 10 GE/ml serum).
[b] Liver biopsy was performed at indicated time-point. p.i., postinoculation; NT, not tested.
[c] Group I, primary infection experiment in which 1-year-old animals were inoculated with two different types of inocula.
[d] Group II, reinfection experiment, where HCV RNA-positive sera from Group I experimental infections were passaged to naive animals.
[e] GroupIII, no-infection control.

ined. In the present study, we describe the clinical development and pathology of HCV-infected tupaias over an approximately 3-year time course.

MATERIALS AND METHODS

Animals. Table 1 summarizes the tupaias used in this study. Tupaias born in laboratory captivity were obtained from the Laboratory Animal Center at the Kunming Institute of Zoology (Chinese Academy of Sciences). Tupaias were imported with permission from the Convention on International Trade in Endangered Species of Wild Fauna and Flora (7), quarantined for medical inspection, and housed individually in standard rat cages supplied with filtered air. The animals were fed a daily regimen of eggs, fruit, and the CMS-1 commercial diet for marmosets (CLEA, Japan). Their appetites and feces were carefully monitored. Animal care and experimental handling conformed to study guidelines established by the Subcommittee on Laboratory Animal Care at the Tokyo Metropolitan Institute of Science.

Patient serum used for animal infection. HCV genotype 1b serum, designated HCR6, was obtained from a patient with chronic active hepatitis C. The infectious titer of HCR6 was determined in chimpanzee and Molt4 cells and denoted plasma K (HCR6) by Shimizu et al. (24). The HCR6 serum exhibited a PCR titer of 6×10^6 genome equivalents/ml and an infectious titer of 3.7×10^4 50% chimpanzee infectious doses/ml. Serum aliquots were frozen at −80°C until they were used.

Virion reconstitution of cloned HCV. As described previously, pHCR6 (genotype 1b; 9,611 nucleotides; GenBank accession no. AY045720) is a plasmid carrying HCV genomic cDNA cloned from HCR6 serum (30). pHCR6Rz was designed for precisely trimmed RNA expression, with the entire genomic region of pHCR6Rz recloned under the control of the T7 promoter and the 5′ and 3′ distal ends flanked by hammerhead- and hepatitis D virus ribozyme-encoding sequences, respectively (22, 25).

For molecular reconstitution of HCV particles, pHCR6Rz was transfected into IMY-N9 cells as described previously (12). Briefly, semiconfluent IMY-N9 cells in 100-mm plastic dishes were transfected with 15 μg of plasmid using 40 μl of cationic lipids (DMRIE-C reagent; Life Technology) in accordance with the manufacturer's instructions. Five hours after transfection, the cells were infected with AdexCAT7 (2) (kindly provided by Y. Matsuura) at a multiplicity of infection of 20. After infection, the culture medium was replaced with Hepato-STIM (Becton Dickinson). The culture supernatants were collected at 24 h postinfection and stored at −80°C.

Virus inoculation and collection of serum samples. Animals were infected at 6 months of age. The anesthetic agent, ketamine hydrochloride, was administered intramuscularly at 50 mg/kg body weight prior to virus inoculation and bleeding of the tupaias. The inocula were introduced intravenously at 6×10^5 genome equivalents/animal for patient serum HCR6 and 1×10^7 genome equivalents/animal for reconstituted virions derived from the pHCR6Rz inoculation. Blood samples were drawn from infected and control animals pre- and postinfection. Briefly, the animals were bled weekly for 20 weeks and biweekly thereafter. At each time point, 0.5 ml of blood was drawn from the thigh vein; the sera were separated, aliquoted, and stored for subsequent assays.

Reinfection experiments were performed by transmission of HCV RNA-positive serum from group I (Table 1) to naive animals.

Serum alanine aminotransferase (ALT) concentrations were determined using a Transnase Nissui kit (Nissui Pharmaceutical Co.), standardized, and displayed as IU/liter.

RNA isolation and quantitative RTD-PCR assay for HCV RNA. Serum samples (100 μl) were tested for circulating HCV RNA in vivo using quantitative real-time detection (RTD)-PCR (TaqMan). RNA was extracted from the sera and livers of sacrificed animals using the acid guanidium-phenol chloroform method with tRNA as a carrier (3). Two tupaias (Tup.5 and Tup.6) were inoculated with patient serum HCR6. Another two animals (Tup.4 and Tup.8) were inoculated with reconstituted viral particles (RCV). Tup.15 served as a mock-infected control. Liver specimens (3- to 4-mm^2 blocks) from these tupaias were homogenized with 1.5 ml of 5 M guanidine thiocyanate using a polytron-type homogenizer (Ultra-Turrax T25; IKA Laborteehnik, Staufen, Germany). RNA was then reextracted with 4 M guanidine thiocyanate.

RNA samples were subjected to RTD-PCR on an ABI 7700 sequence detector (Applied Biosystems) as described previously (26). The extracted RNA was dissolved in 200 μl of diethyl pyrocarbonate-treated water containing 10 mM dithiothreitol and 200 units/ml RNase inhibitor in a siliconized tube. RTD-PCR was performed using 1 μg of total RNA, one set of PCR primers, and a probe for a location within the 5′ noncoding region using the EZ *rTth* RNA PCR kit (Perkin Elmer) and the ABI Prism 7700 sequence detector system. A standard curve was constructed using a 10-fold dilution series of in vitro-transcribed and previously titrated synthetic HCV RNA.

Consequently, the quantities represented by genome equivalents correspond to an absolute standard curve (26). All quantitative RTD-PCR assays were performed using duplicate samples, with both negative control serum and HCV-positive serum included. The control sera were diluted before use and were estimated to contain low copy numbers of HCV RNA (100 genome equivalents/ml serum). Samples were deemed positive for HCV RNA if both duplicates yielded PCR-amplified product. Averages of the two estimated values are shown in the figures.

Histological analysis. Tissue samples were carefully collected from anesthetized animals by abdominal incision, fixed in 10% neutral buffered formalin, embedded in paraffin, sectioned, and stained with hematoxylin and eosin (H&E). Silver and Sudan IV (Wako Pure Chemical Industries, Ltd.) staining were also carried out to visualize fiber generation and lipid degeneration, respectively. All histological staining was performed in accordance with conventional procedures. The histological status was determined using the modified hepatitis activity index scoring system, which grades necrosis and inflammation on a scale of 0 to 18 (periportal inflammation and necrosis, 0 to 10; lobular inflammation and necrosis, 0 to 4; portal inflammation, 0 to 4) (11). Fibrosis was scored using the Ishak fibrosis scale of 0 to 6 (0, no fibrosis; 1 or 2, portal fibrosis; 3 or 4, bridging fibrosis; and 5 or 6, cirrhosis). The values in each group (Table 2) represent the averages of the scores in five visual fields.

Statistical analysis. The statistical significance of differences between controls and HCV-infected animals was analyzed with the nonparametric Mann-Whitney U test. All comparisons were two tailed. The statistical analysis was conducted with SPSS 12.0 software (SPSS Inc., Chicago, IL).

RESULTS

Inoculation of HCV causes acute hepatitis and transient viremia in tupaias. To begin this study, two distinct but related inocula were chosen for infection of tupaias. Serum from a chronic hepatitis patient (designated HCR6) was chosen for its

TABLE 2. Grading: necroinflammatory scores and fibrosis

Group	Inoculum	Tupaia no.	Grade				Total	Avg	SD	Staging
			A	B	C	D				
94 wk p.i. (biopsy)										
I	HCR 6	Tup.5	0	0	0	0	0	1.3	1.5	0
		Tup.6	1	0	1	0	2			0
	RCV	Tup.4	0	0	0	0	0			0
		Tup.8	0	0	0	3	3			6
	Control	Tup.15	0	0	0	0	0	0	0	0
III		Tup.17	0	0	0	0	0			0
		Tup.38								
		Tup.39								
144 wk p.i. (sacrifice)										
I	HCR 6	Tup.5	1	0	2	3	6	5.5	3.7	0
		Tup.6	3	0	4	3	10			1
	RCV	Tup.4	0	0	0	1	1			0
		Tup.8	1	0	1	3	5			6
	Control	Tup.15						0	0	
III		Tup.17								
		Tup.38	0	0	0	0	0			0
		Tup.39	0	0	0	0	0			0

defined genotype (genotype 1b), and genetic heterogeneity was ascertained by the process of cloning consensus cDNA. The infectivity of this serum was also experimentally defined in chimpanzees; a 50% chimpanzee infectious dose was estimated at 3.7×10^4 50% chimpanzee infectious doses/ml. Furthermore, the consensus genomic sequence of HCV was cloned from the serum (pHCR6; 9,611 bases; GenBank AY045702.1). For the second inoculum (referred to as RCV), clonal viral particles were reconstituted as described in Materials and Methods. This inoculum was expected to be free of neutralizing antibodies and thus was considered potentially more infectious than patient sera. In the case of RCV infection, genetic diversification of viral RNA, also known as quasispecies, can be regarded as a direct indication of de novo synthesis of progenitor virus in vivo.

Either patient serum or cDNA-derived RCV was inoculated into tupaias (Table 1, group I). Two animals (one female and one male) were tested against each inoculum. Age-matched animals were bred as infection-free controls.

All experimental infections are described in Materials and Methods and Table 1. Prior to experimental infection, the normal serum ALT level in tupaias was measured at 22.3 IU/liter ($n = 23$).

Inoculation with patient serum HCR6 caused rapid fluctuations in the serum ALT concentrations, from two- to fivefold, in both inoculated tupaias, suggesting acute hepatitis in vivo (Fig. 1A and B). Correlative quantitative RTD-PCR revealed HCV viremia soon after serum inoculation in Tup.5, which continued to show transient viremia long term. The appearance of viremia sometimes coincided with a steep elevation in the serum ALT (Fig. 1A). Conversely, HCV RNA was not detected in the serum of Tup.6 up to 60 weeks postinoculation and only twice thereafter. Acute-phase ALT elevations (3 to 4 weeks postinoculation) in Tup.6 might represent tight control of HCV infection by the host immune system (Fig. 1B).

Distinct results were obtained for the two animals (Tup.4 and Tup.8) inoculated with RCV. Both animals displayed sustained viremia up to 10 weeks postinoculation (Fig. 1C and D), indicating persistent HCV infection and inability to eradicate the virus. Viremia was detected intermittently throughout the course of infection, sometimes accompanying the elevation of serum ALT. Humoral immune responses in Tup.5 and Tup.6 (see Fig. S1A in the supplemental material) and Tup.4 and Tup.6 (see Fig. S1B in the supplemental material) were indicated.

We performed RTD-PCR to confirm whether HCV could replicate in the tupaias' livers (Tup.4, Tup.5, Tup.6, and Tup.8) and obtained the following results (Fig. 1E): 310 ± 117 copies/μg total RNA in Tup.5, 80 ± 11 copies/μg in Tup.6, 199 ± 77 copies/μg in Tup.4, and 292 ± 48 copies/μg in Tup.8. In contrast, HCV RNA was not detected in the liver of the mock-infected animal (Tup.15).

HCV RNA was also not detected in samples from either preinoculation or age-matched, infection-free control tupaias (Table 1, group III), nor were significant elevations in serum ALT observed for any of the three infection-free controls (data not shown).

HCV causes chronic hepatitis in tupaia liver, leading to fibrosis and cirrhosis. Serum ALT and circulating HCV RNA levels in primary infected tupaias (Table 1, group I) were monitored for 3 years postinoculation. As described above, the magnitudes of serum ALT fluctuations varied substantially among infected animals (Fig. 1A, B, C, and D). Tupaia livers were examined for histological lesions in order to elucidate if HCV caused chronic hepatitis. Liver biopsies via abdominal incisions were performed at 2 years postinoculation. All animals were sacrificed at 3 years postinoculation (4.5 years for uninfected animals). H&E staining of liver specimens from HCV-infected tupaias showed infiltrating lymphocytes within sinusoids and around portal areas, indicating chronic hepatitis in the tupaia livers (Fig. 2B, D, and H). Infiltrating lymphocytes were also observed in limiting plates, indicating ongoing inflammation (Fig. 2G and H). Furthermore, a comparison of liver samples at 2 and 3 years postinoculation revealed that the

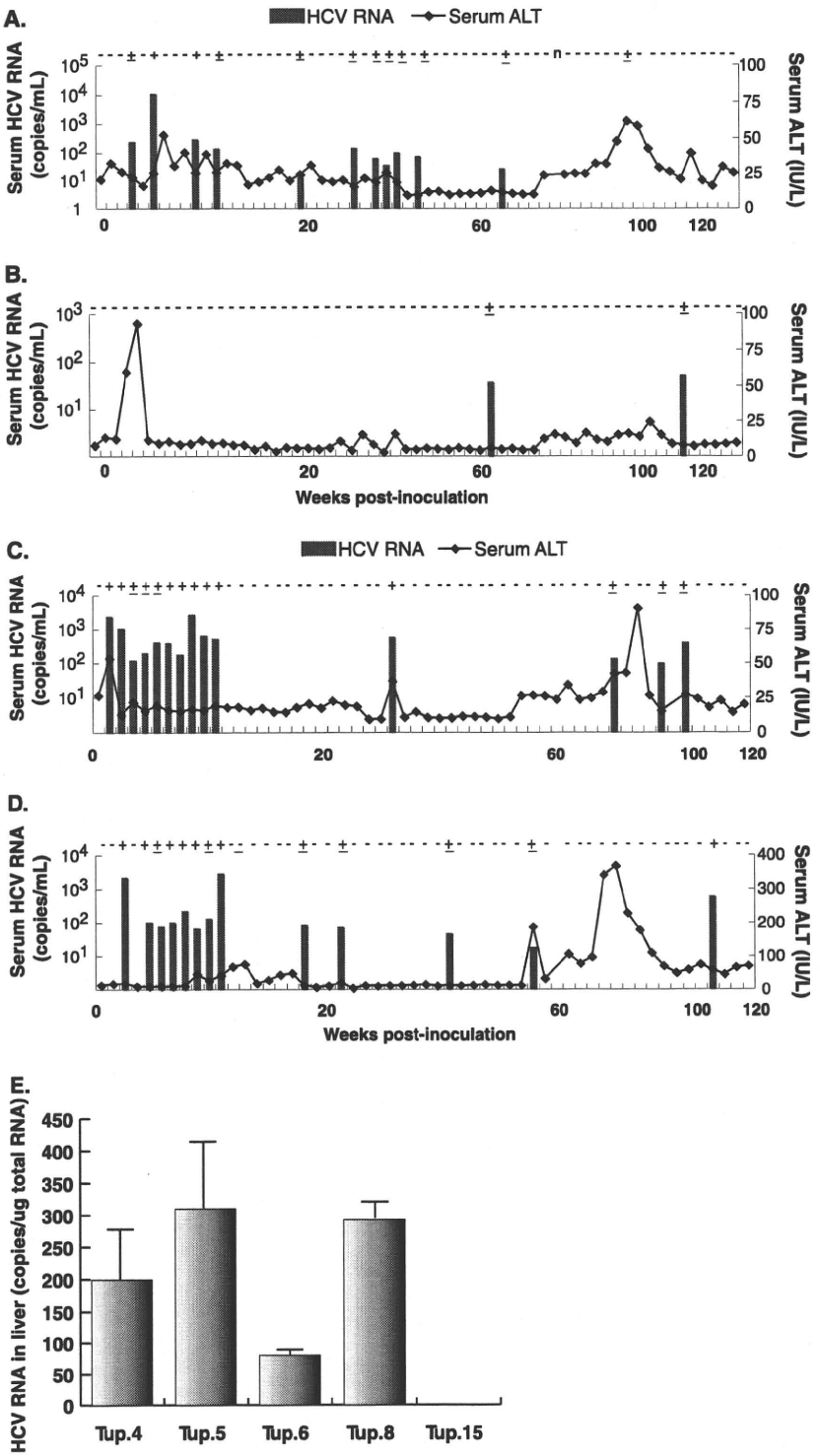

FIG. 1. Course of infection with patient serum HCR6 and RCV. (A) The results of quantitative RTD-PCR for HCV RNA and serum ALT concentrations were combined and plotted to show the course of infection in Tup.5. The bars and the ordinates on the left represent HCV RNA as genome equivalents/ml of serum. The curved line and the ordinates on the right represent serum ALT concentrations as IU/liter serum. (B) Serum HCV RNA and ALT concentrations for infection of Tup.6. (C) The graph for Tup.4. (D) The graph for Tup.8. The vertical axis for serum ALT in this graph is scaled differently from the others because of significant ALT elevation. (E) Quantification of HCV RNA in tupaia liver. HCV RNA in hepatocytes from tupaia (Tup.4, Tup.5, Tup.6, Tup.8, and Tup.15) livers was isolated 172 weeks after HCV infection and quantified by RTD-PCR. As few as 10 copies of the genome were detected, and the quantification range was between 10^1 and 10^8 copies (26).

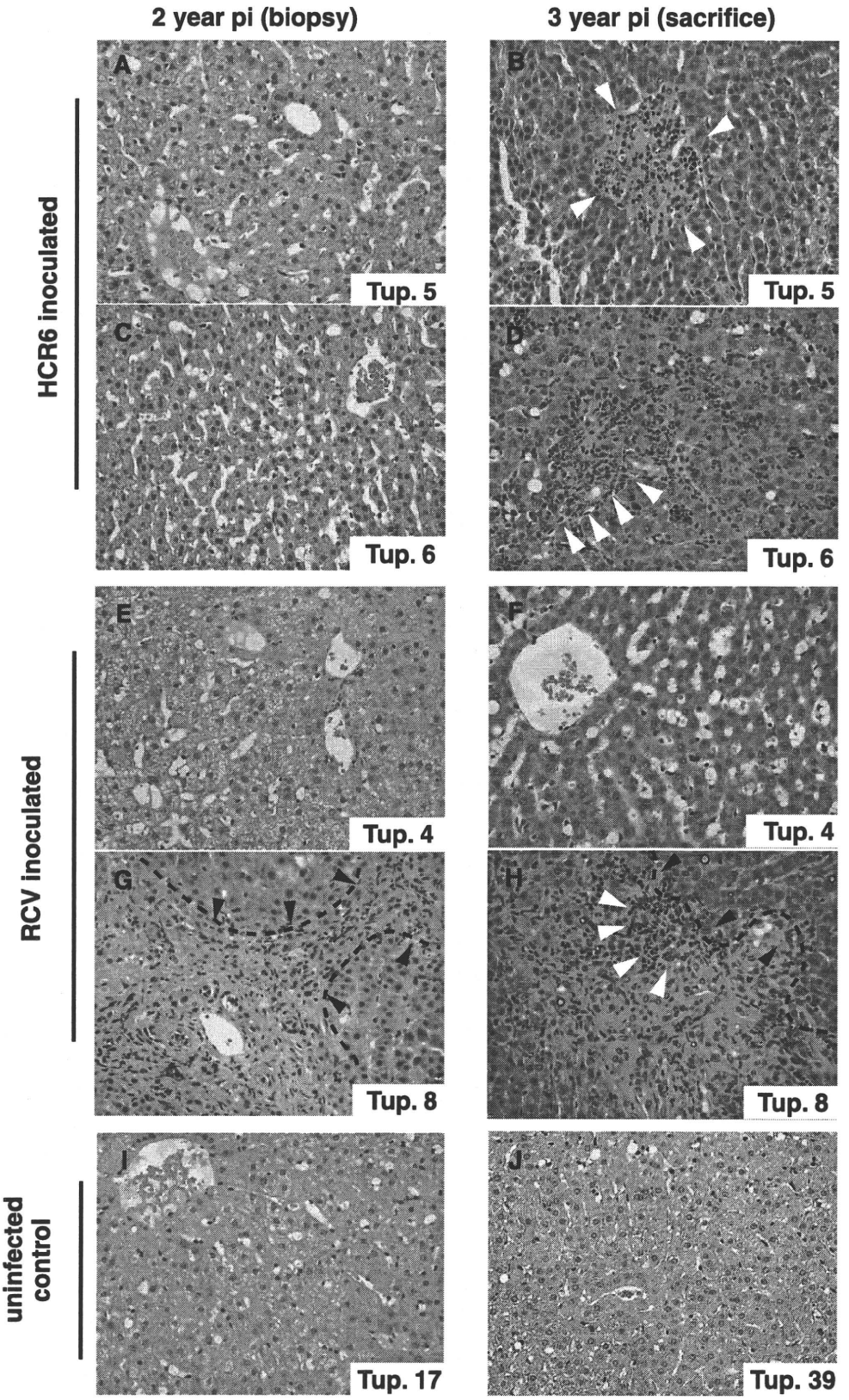

FIG. 2. Micrographs of liver specimens stained with H&E. Liver tissue from HCR6-inoculated tupaias (A to D) and RCV-inoculated tupaias (E to H) was obtained at 2 and 3 years postinoculation (pi). (I and J) Liver specimens from uninfected animals age matched to each inoculated animal were also obtained. The HCV-infected tupaia livers harbored infiltrating lymphocytes (white arrowheads) and fibrosis (broken lines and black arrowheads), which indicate chronic hepatitis.

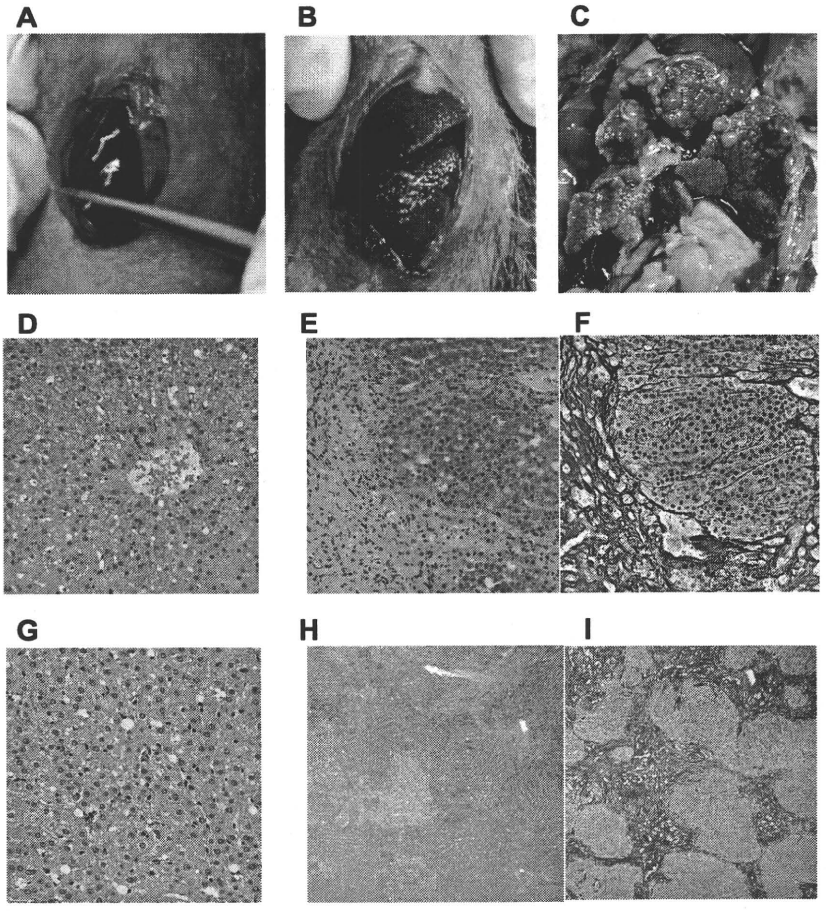

FIG. 3. Macro- and microscopic features of tupaia liver. (A) Infection-free control tupaia (Tup.15; 92 weeks). (B) RCV-infected animal displaying liver cirrhosis (Tup.8; 84 weeks postinoculation). (C) RCV-infected animal with massive surface nodules (Tup.8; 144 weeks postinoculation). (D and G) H&E staining of the uninfected Tup.15 at 92 weeks (D) and the uninfected Tup.39 at 242 weeks (G). (E, F, H, and I) H&E and silver staining of Tup.8 at 84 weeks postinoculation (E and F) or at 144 weeks postinoculation (H and I).

hepatitis had worsened with time in all HCV-infected tupaias (Fig. 2A to H and Table 2).

Fibrosis and cirrhosis were also examined. Mild fibrosis was seen in Tup.6, while severe fibrosis was seen in Tup.8. Cirrhosis was histologically investigated in all animals (Table 2). There was no significant difference between groups I and III at 94 weeks postinfection ($P = 0.194$), but at 144 weeks postinfection, a slight difference was observed ($P = 0.059$; SPSS 12.0). Macroscopic observation of the liver biopsy specimens (taken 2 years postinoculation) indicated liver cirrhosis in Tup.8 (Fig. 3B) compared with Tup.15 (uninfected control) (Fig. 3A), while silver staining of histology samples revealed fibrosis and cirrhotic nodules (Fig. 3E and F). Macroscopic observation upon sacrifice (3 years postinoculation) indicated that liver cirrhosis in Tup.8 had worsened (Fig. 3C). In contrast, age-matched infection-free negative control tupaias displayed none of these pathologies (Fig. 3A, D, and G).

Progressive lipid degeneration was noted in infected tupaias throughout the course of infection (Fig. 4). In particular, Tup.5 displayed microvesicular lipid droplets in the first biopsy specimens (at 2 years), which developed into macrovesicular droplets and foamy degeneration in biopsy specimens at 3 years (Fig. 4C and D). Liver specimens from other infected animals displayed intracellular micro- and macrovesicular lipid droplets in hepatocytes at 3 years postinoculation (Fig. 4F, H, and J). These anomalies were not present in liver specimens from infection-free control animals (Fig. 4A and B).

Transmission of viral-RNA-positive serum to naive animals reproduces acute hepatitis and viremia. To confirm virion regeneration in vivo, and to exclude the possibility of false-positive serum HCV RNA results due to amplification of the original inocula, HCV RNA-positive sera from primary inoculated tupaias were used to inoculate naive tupaias. Three different sera were tested in this passage experiment, with two naive tupaias used as recipient animals for each trial (see Materials and Methods) (Table 1, group II).

In the first reinfection experiment, serum from Tup.5 (originally infected with patient serum HCR6) was collected at 5 weeks postinoculation and used to infect two naive animals. The recipient animals showed intermittent viremia over the subsequent 3 months (Fig. 5A). In the second and third cases of reinfection, sera from Tup.8 at 10 weeks postinoculation and from Tup.4 at 8 weeks postinoculation also induced viremia in the naive inoculated animals, similar to the first reinfection experiment (Fig. 5B and C). Furthermore, the PCR titers of the recipient tupaias were significantly greater than the inoc-

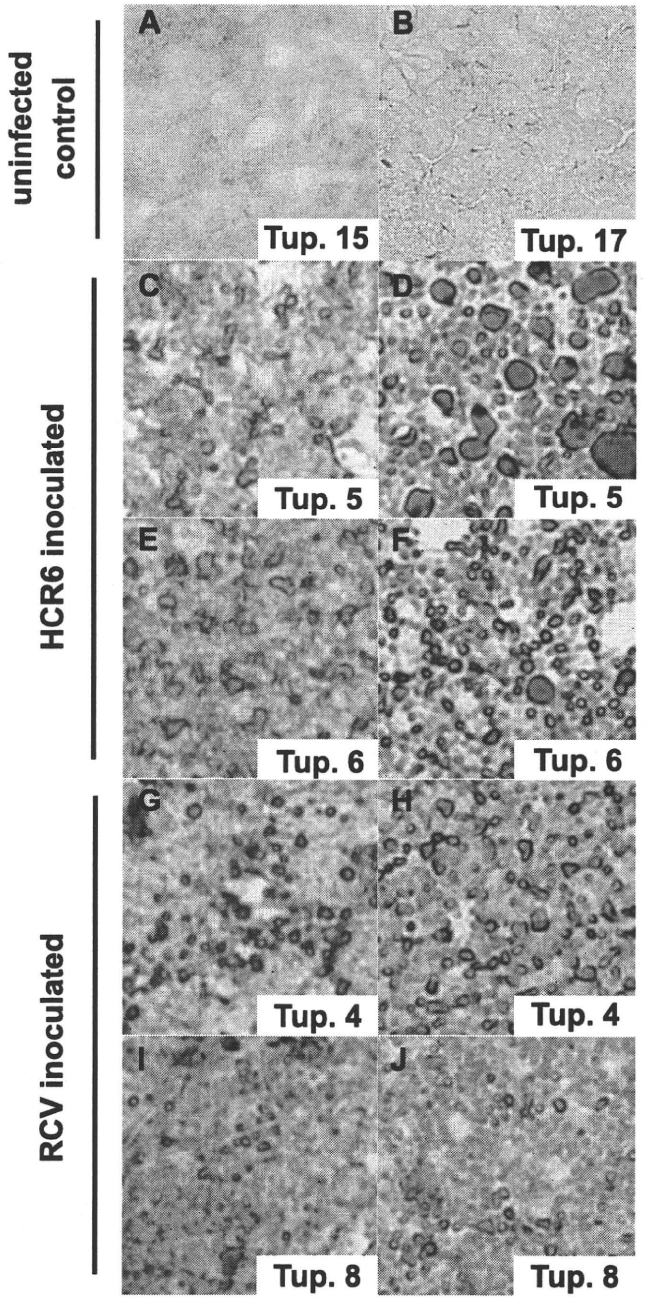

FIG. 4. Sudan IV-stained liver specimens exhibiting fatty liver degeneration. Cryosections of liver stained by Sudan IV as described in Materials and Methods show fatty liver degeneration. The left and right columns display biopsy specimens of infected animals (2 years postinoculation) and animals sacrificed at 3 years postinfection, respectively. (A and B) Uninfected controls at 2 years (Table 1 shows sample timing). (C to F) Patient serum HCR6-infected animals. (G to J) RCV-infected animals.

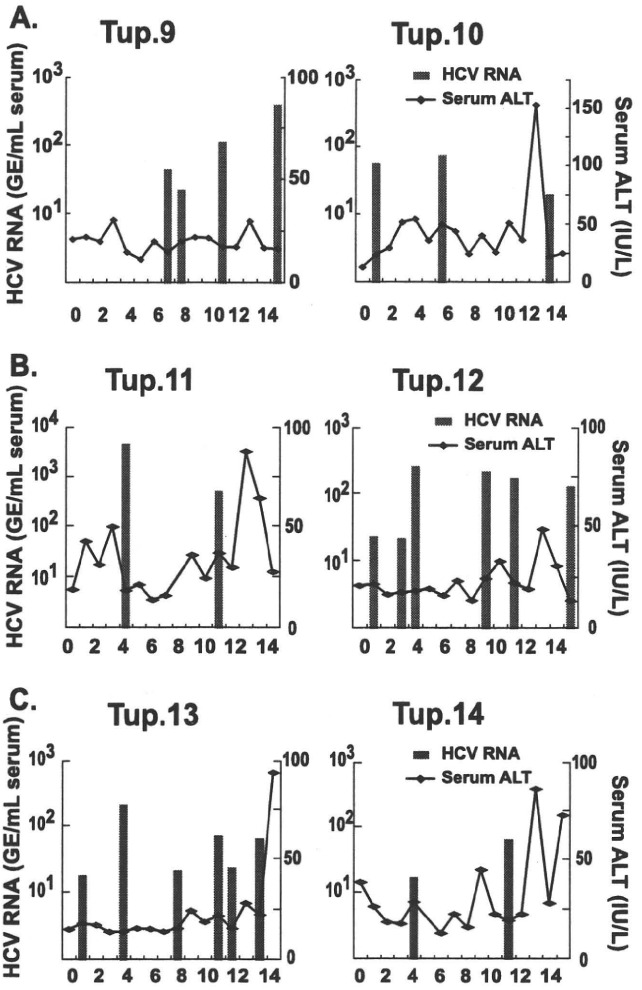

FIG. 5. Results of a reinfection experiment. (A) Quantitative RTD-PCR for HCV RNA and serum ALT levels are shown. Two naive animals were inoculated with tupaia serum (using serum taken at 5 weeks postinoculation from Tup.5, originally inoculated with patient serum HCR6) containing 100 genome equivalents (GE)/ml and were monitored for 15 weeks postinoculation (Table 1). (B) Tupaia serum (taken at 10 weeks postinoculation from Tup.8, originally inoculated with RCV) that was positive for HCV RNA was passaged into two naive animals. The animals were inoculated with tupaia serum at 100 GE/animal and monitored for 15 weeks postinoculation. (C) Tupaia serum (taken at 8 weeks postinoculation from Tup.4, originally inoculated with RCV) that was positive for HCV RNA was passaged into naive animals. The animals were inoculated with serum at 100 GE/animal and monitored for 20 weeks postinoculation.

ulation titers (10^2 genome equivalents/animal) (Table 1). For Tup.11, serum from 4 weeks postinoculation contained almost 10^4 genome equivalents/ml of HCV RNA (Fig. 5B). In addition, significant increases in serum ALT accompanied detection of serum HCV RNA. These results indicate that HCV RNA-positive sera from group I actually contained infectious virion particles. They also suggest that reconstituted HCV particles made from cDNA are infectious in tupaias.

We amplified a portion of the NS5A sequence, which is known as the interferon sensitivity determining region, by reverse transcription-PCR as described in the supplemental material. Each PCR product was subcloned and sequenced to compare the encoded amino acid sequences. For the purposes of this study, animals were inoculated with a molecular clonal virus consisting of a unique viral sequence of cDNA. The interferon sensitivity determining region sequences recovered from an animal infected with clonal inoculum (Tup.8 at 103 weeks postinoculation) were found to be heterogeneous, with